Chinese Chemical Letters 33 (2022) 653–662

Contents lists available at ScienceDirect

Chinese Chemical Letters

journal homepage: www.elsevier.com/locate/cclet

Recent advances and trends of heterogeneous electro-Fenton process for wastewater treatment-review

Zining Wang[a], Mingyue Liu[a], Fan Xiao[a], Georgeta Postole[b], Hongying Zhao[a,*], Guohua Zhao[a]

[a] School of Chemical Science and Engineering, and Shanghai Key lab of Chemical Assessment and Sustainability, Tongji University, Shanghai 200092, China
[b] Univ Lyon, Université Claude Bernard Lyon 1, CNRS, IRCELYON, F-69626 Villeurbanne, France

ARTICLE INFO

Article history:
Received 30 April 2021
Revised 14 June 2021
Accepted 16 July 2021
Available online 23 July 2021

Keywords:
Heterogeneous electro-Fenton
Oxygen reduction reaction
Hydrogen peroxide
Cathodic materials
Refractory organic pollutants

ABSTRACT

Electrochemical advanced oxidation processes (EAOPs) are effective and environmentally friendly for the treatment of refractory organic pollutants. Among EAOPs, heterogeneous electro-Fenton (EF) process with *in-situ* formation of hydrogen peroxide (H_2O_2) is an eco-friendly, cost-effective and easy-operable technology to generate hydroxyl radicals ($^{\bullet}OH$) with high redox potential. The generation of $^{\bullet}OH$ is determined by the synergistic H_2O_2 formation and activation. The surface catalytic mechanisms for H_2O_2 activation in the heterogeneous EF process were discussed. Some required features such as heteroatom doping and oxygen groups for H_2O_2 formation via selective two-electron oxygen reduction reaction (ORR) with carbonaceous electrode are summarized. The solid Fenton catalysts and integrated functional cathodes that widely used in heterogeneous EF for wastewater treatment are grouped into few classes. And the brief discussion on catalytic activity and stability of materials over different experimental conditions are given. In addition, the application of heterogeneous EF process on the remediation of emerging contaminants is provided. The challenges and future prospects of the heterogeneous EF processes about catalytic fall-off and multi-step/complex techniques for water purification are emphasized.

1. Introduction

Nowadays, with the rapid development of economy and the explosive growth of population, the environmental pollution became an urgent global issue. Various emerging organics are frequently detected in urban sewage, drinking water surface and ground water, including dyes [1], endocrine disrupting chemicals (EDCs) [2–4], pesticides [5–7], pharmaceutical and personal care products (PPCPs) [8–11]. Although the concentration of organics and corresponding degradation intermediates is the order of ng/L to μg/L, such contaminants with stable chemical properties are highly cytotoxic, persistent and intractable [12–14]. Furthermore, after continuous accumulation and enrichment, the presence of refractory organics would cause serious pollution to water environment, and then gradually results in a potential threat to human life and health through the food chain [15,16].

As an environmentally friendly advanced oxidation technology, electrochemical advanced oxidation processes (EAOPs) are promising and efficient methods for the elimination of organic pollutants. The most obvious feature of EAOPs is the production of strong oxidant hydroxyl radical ($^{\bullet}OH$, E^0 ($^{\bullet}OH/H_2O$) = 2.80 V), which can efficiently and unselectively attack a wide range of organics [17–21]. Electro-Fenton (EF) is one of the most widely used technology in EAOPs for wastewater treatment due to its fast reaction rate, low toxicity and environmental compatibility [22]. In EF process, the H_2O_2 is continuously generated *via* the two-electron oxygen reduction reaction, avoiding the risk of long-distance transportation of H_2O_2. The electrogenerated H_2O_2 would react with external added ferrous ions (Fe^{2+}) to produce $^{\bullet}OH$. Depending on the types of the Fenton catalysts, EF process can be divided into heterogeneous and homogeneous reaction [19,23]. In homogeneous EF process, the Fenton catalysts are Fe^{2+} ions which react with the *in-situ* generated H_2O_2 *via* (Eq. 1). The catalytic efficiency of homogenous EF process is determined by the regeneration of Fe^{2+} (Eq. 2). Indeed, the rapid accumulation of Fe^{3+} and the slow rate of the Fe^{2+} regeneration result in low efficiency of decomposing H_2O_2 as well as undesirable precipitation of iron oxyhydroxides. The requirement of strong acidic conditions (pH 2.8–3.5) for achieving optimal efficiency limits its large-scale application for actual wastewater treatment, which needs final neutralization step to obtain tol-

* Corresponding author.
E-mail address: hyzhao@tongji.edu.cn (H. Zhao).

https://doi.org/10.1016/j.cclet.2021.07.044
1001-8417/

erable effluents [24,25].

$$Fe^{2+} + H_2O_2 \rightarrow Fe^{3+} + {}^{\bullet}OH + OH^- \quad \left(k_1 = 40 \sim 80\,L\ mol^{-1}\,s^{-1}\right) \tag{1}$$

$$Fe^{3+} + H_2O_2 \rightarrow Fe^{2+} + HO_2^{\bullet} + H^+ \quad (k_2 = 9.1 \times 10^{-7}\,L\ mol^{-1}\,s^{-1}) \tag{2}$$

Recently, heterogeneous EF technology by using solid catalysts or integral cathodes receives intensive research and development focus due to its environmental compatibility, excellent efficiency, and high versatility. Considering the main problems of homogeneous EF process, the most important advantages of heterogeneous EF are the extension of working pH range and the inhibition of iron sludge formation during heterogeneous EF process [26,27]. In particular, Fe-containing synthetic solid catalysts (*i.e.*, pyrite, iron oxides and spinel) are used alone or supported on the porous materials for the application in heterogeneous EF process. Of recent, functionalized cathodic materials (*i.e.*, Fe-modified carbon/graphite felt and transition metal doped carbon aerogel) are directly applied as working electrodes in heterogeneous EF process [28–31]. The application of heterogeneous catalysts or cathodic materials can be efficiently recovered and reused, the overall cost of wastewater treatment can be reduced.

Hence, many studies have already been carried out concerning about the heterogeneous EF process for the remediation of wastewater. These processes can efficiently degrade and even mineralize real and synthetic wastewater contaminated by pesticides, dyes, endocrine disrupting chemicals, antibiotics, *etc.* [32,33]. Up to now, in several reviews and book chapters, few reviews have comprehensively introduced the cathodic reaction mechanism, cathodic materials as well as the application of heterogeneous EF process. Thus, the selectively electrochemical mechanism of oxygen reduction reaction for H_2O_2 generation and H_2O_2 decomposition in the heterogeneous EF process were emphasized in this review. Different heterogeneous Fenton catalysts and functional cathodic materials and their application in the degradation of emerging contaminants were discussed. The current challenges and future trends were also proposed from the perspective of reactive oxygen species (ROS) generation and actual water purification application.

2. The main features and surface catalytic mechanism of heterogeneous electro-Fenton processes

The heterogeneous EF process is conducted with *in-situ* electrogenerated H_2O_2 and solid Fenton catalyst to form $^{\bullet}OH$, which promotes the effective mineralization and removal of pollutants. Considering the security issues related to the storage and transportation of H_2O_2, the electrogeneration of H_2O_2 *via* two-electron reduction of input air or oxygen, which can avoid the costs and risks associated with handling, transportation and storage of H_2O_2 [9,34]. Heterogeneous electro-Fenton process has some significant advantages over classical electro-Fenton process such as extending the working pH range, preventing the iron ions leaching, increasing the stability and reusability of catalysts. When applied in a wide pH window, the formation of iron hydroxides sludge during hetero-EF process or post-treatment neutralization stage can be eliminated or inhibited. This is important because the elimination of sludge could improve the efficiency of the process as well as reduce both overall cost and energy consumption [28,35].

Most researchers propose that the catalytic hetero-EF reaction consists of the Haber-Weiss circle mechanism. In the surface-induced decomposition of electrogenerated H_2O_2 is mainly catalyzed by surface iron species (≡indicates surface-bound iron species in heterogeneous catalyst, as shown in Fig. 1). At the acidic working pH conditions, the decomposition mechanism of H_2O_2 on the solid catalyst surface is simplified as shown in (Eqs. 3–5). $\equiv Fe^{II}$ on the surface of the solid catalyst efficiently decompose H_2O_2 to form $^{\bullet}OH$, and at the same time itself oxidizes to $\equiv Fe^{III}$ as the (Eq. 3). In addition, hetero EF process may accompany the dissolved Fe^{3+}/Fe^{2+} released from the Fe-functionalized cathodic materials or solid catalysts, the reaction mechanism is similar to the homogeneous EF (Eq. 4). Finally, through $^{\bullet}OH$ attacking, the organic pollutants can be mineralized to H_2O and CO_2 (Eq. 5). The $^{\bullet}OH$ can also react with excess H_2O_2 to generate $HO_2^{\bullet}$ (quenching Eq. 6). Compared with $^{\bullet}OH$, $HO_2^{\bullet}$ is a much weaker oxidant, hence the efficiency of the process will be reduced [36,37].

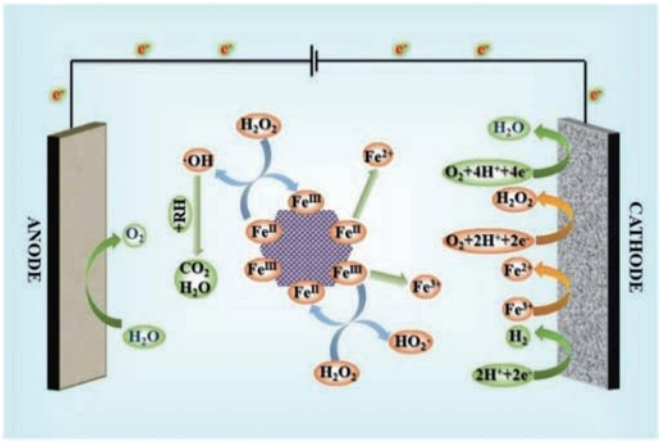

Fig. 1. Diagram of degradation mechanism for organic matter by heterogeneous electro-Fenton oxidation.

$$\equiv Fe^{II} + H_2O_2 \rightarrow \equiv Fe^{III} + {}^{\bullet}OH + OH^- \tag{3}$$

$$Fe^{2+} + H_2O_2 \rightarrow Fe^{3+} + {}^{\bullet}OH + OH^- \tag{4}$$

$$^{\bullet}OH + \text{organic pollutants} \rightarrow \text{byproducts} \rightarrow CO_2 + H_2O \tag{5}$$

$$^{\bullet}OH + H_2O_2 \rightarrow OH_2^{\bullet} + H_2O \tag{6}$$

In natural or alkaline condition, a different surface catalyzed mechanism was proposed in (Eqs. 7–11). Initially, the electrogenerated H_2O_2 prefers to bind with the $\equiv Fe^{II}$-OH/$\equiv Fe^{III}$-OH active sites of the iron based catalysts (Eqs. 7 and 8), forming a precursor surface complex $\equiv Fe^{II}\text{-}OH(H_2O_2)_{(s)}/\equiv Fe^{III}\text{-}OH(H_2O_2)_{(s)}$. Furthermore, $\equiv Fe^{II}\text{-}OH(H_2O_2)_{(s)}$ in catalysts surface catalyzes the decomposition of adsorbed H_2O_2 into $^{\bullet}OH$ radicals and converted them to $\equiv Fe^{III}$-OH during the reaction (Eq. 9). Then the surface H_2O_2 complex may transfer into $\equiv Fe^{II}\text{-}OH(HO_2^{\bullet})_{(s)}$ through a reversible ground-state electron form the ligand to the central atom (Eq. 10), and then the successor complex would be activated to $\equiv Fe^{II}$-OH through (Eq. 11). Obviously, the reaction rates of the (Eq. 10) can be significantly accelerated by increasing the pH value to the alkaline condition, because the rapid consumption of H^+ will rapidly change the equilibrium, resulting in the formation of more $\equiv Fe^{II}$-OH species. This cycle will continue to convert electrogenerated H_2O_2 to $^{\bullet}OH$ radicals [38–40] .

$$\equiv Fe^{II} - OH + H_2O_2 \rightarrow \equiv Fe^{II} - OH(H_2O_2)_s \tag{7}$$

$$\equiv Fe^{III} - OH + H_2O_2 \rightarrow \equiv Fe^{III} - OH(H_2O_2)_{(s)} \tag{8}$$

$$\equiv Fe^{II} - OH(H_2O_2)_{(s)} \rightarrow \equiv Fe^{III} - OH + OH^- + {}^{\bullet}OH \tag{9}$$

$$\equiv Fe^{III} - OH(H_2O_2)_{(s)} \rightarrow \quad \equiv Fe^{II} - OH(HO_2^{\bullet})_{(s)} + H^+ \tag{10}$$

$$\equiv Fe^{II} - OH(HO_2^{\bullet})_{(s)} \leftrightarrow \equiv Fe^{II} - OH + HO_2^{\bullet} \tag{11}$$

As we have known, the regeneration of Fe^{II} from Fe^{III} dictates the performance of the whole heterogeneous electro-Fenton reaction, represented by the amount of produced $^{\bullet}OH$. During the heterogeneous EF reaction, surface $\equiv Fe^{III}$ can be reduced to $\equiv Fe^{II}$ with H_2O_2 and $HO_2^{\bullet}$ by the following reactions (Eqs. 12 and 13). However, the regeneration rate of Fe^{II} is very slow with the rate constant of 0.001–0.01 L $mol^{-1}s^{-1}$, which is far less than of generation rate constant of Fe^{III} (40-80 L $mol^{-1}s^{-1}$) [41,42]. The adopted strategy for enhancing the regeneration of Fe^{II} is the addition of cocatalysts such as inorganic metal compounds and organic acids. Most organic acids act as chelating and reducing agents to provide extra electrons for Fe^{III} complexes and promote Fe^{II} cycling [3,43]. Inorganic metal compounds have been used to introduce a thermodynamically spontaneous Fe^{II} regeneration *via* the synergistic effect of other metals and Fe with different redox potentials [44,45]. Besides, the current research indicates that the catalyst structure adjustment to accelerate catalyst interface electronic migration and circulation mainly include several aspects, metal and metal oxide compound, different types of metal oxide compound and the use of nonmetal materials with good conductivity (such as graphene) as the carrier of metal components *etc* [40,46–48]. Furthermore, the regeneration of Fe^{II} can be directly accelerated by using electrochemical reduction method with functional electrode as reducing agent through (Eqs. 14 and 15). Carbonaceous electrodes with heteroatom doping to modify the surface and electronic structures can improve their electrocatalytic activity to realize regeneration Fe^{II} [39,49].

$$\equiv Fe^{III} + H_2O_2 \rightarrow \equiv Fe^{II} + HO_2^{\bullet} + H^+ \tag{12}$$

$$HO_2^{\bullet} + \equiv Fe^{III} \rightarrow \equiv Fe^{II} + H^+ + O_2 \tag{13}$$

$$\equiv Fe^{III} - OH + e^- \rightarrow \equiv Fe^{II} - OH \tag{14}$$

$$Fe^{III} + e^- \rightarrow Fe^{II} \tag{15}$$

3. Selectively electrochemical mechanism of oxygen reduction reaction in heterogeneous electron-Fenton process

Due to its unique characteristics, H_2O_2 has become a versatile and green agent for environmental remediation applications. In heterogeneous EF process, H_2O_2 can be generated through selective oxygen reduction reaction (ORR), which contains two types of reaction pathway: (i) Two-electron reduction as main reaction (Eqs. 16,18,20) and (ii) four-electron reduction as competitive reaction (Eqs. 17,19) [50–52]. Moreover, the reaction equation for selective ORR under different pathway and pH conditions is as follows [53].

In acid media (pH < 7):

$$O_2 + 2H^+ + 2e^- \rightarrow H_2O_2, \quad E^0 = 0.70\ vs.\ \text{RHE} \tag{16}$$

$$O_2 + 4H^+ + 4e^- \rightarrow H_2O, \quad E^0 = 1.23\ vs.\ \text{RHE} \tag{17}$$

In basic media (7 < pH < 11.7)

$$O_2 + H_2O + 2e^- \rightarrow H_2O_2 + 2OH^-, \quad E^0 = 0.70\ vs.\ \text{RHE} \tag{18}$$

$$O_2 + H_2O + 4e^- \rightarrow 4OH^-, \quad E^0 = 1.23\ vs.\ \text{RHE} \tag{19}$$

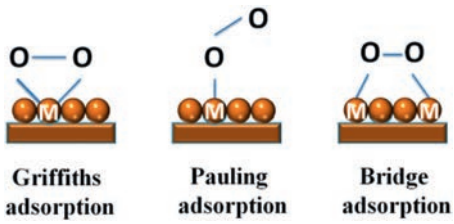

Fig. 2. The oxygen molecule adsorption on the catalyst surface.

At pH>11.7

$$O_2 + H_2O + 2e^- \rightarrow HO_2^- + 2OH^-, \quad E^0 = 0.76\ vs.\ \text{RHE} \tag{20}$$

where RHE represents reversible hydrogen electrode

In order to regulate the reduction pathway of ORR during EF process, it is important to elucidate the ORR mechanism. There are two steps process in $2e^-$ ORR for the production of H_2O_2 which involved proton-coupled electron transfer and the generation of HOO* intermediate on actives site [54]. The first step consists of the adsorption of O_2 molecule on the active sites of catalyst, followed by its reaction with an H^+ and an electron transfer to form a HOO** intermediate (Eq. 21). In the second step, the HOO* intermediate reacts with another H^+ to complete the two-electron path and form H_2O_2 (Eq. 22). The $2e^-$ ORR involves the HOO* as intermediate species, hence, single-electron reduction of HOO* may lead to selective production of H_2O_2, which inhibits further reduction to H_2O [55–57].

$$O_2 + H^+ + * + e^- \rightarrow HOO^* \tag{21}$$

$$HOO^* + H^+ + e^- \rightarrow * + H_2O_2 \tag{22}$$

where * represents the active site on the catalyst surface.

According to the above-mentioned ORR mechanism, the reaction pathway is related to the adsorption mode of O_2 on the surface of electrode. Three adsorption modes of oxygen can be summarized in Fig. 2, including griffiths, Pauling and bridge adsorption [58–60]. In the reduction of O_2 to H_2O_2 through $2e^-$ transfer mechanism, O_2 is "end-on" adsorbed by Pauling mode. During Pauling mode adsorption, only one oxygen atom interacts with the surface activate site, which is conducive to form HOO* intermediate, beneficial to the realization of $2e^-$ reduction of oxygen to generate H_2O_2. In Griffiths model, O_2 molecule transversely interacts with an active site, which can weaken the O–O bonding and further benefit to $4e^-$ ORR pathway. Bridge adsorption, known as "side-on" adsorption, favors the interaction between oxygen atoms and active sites, which is favorable for $4e^-$ ORR pathway. In conclusion, the adsorption modes of O_2 on the surface of electrode play a decisive role in the determination of ORR pathway [53,61,62]. In addition, the binding energy between electrode and O_2 molecules has a significant effect on the ORR activity. Obviously, the binding strength between the electrode and the adsorbed reactants, intermediates or products, should be neither too weak nor too strong. The moderate binding energy of the oxygen-containing species, the better ORR activity [63,64].

Another major problem is selectivity issue, there are a number of side reactions that can occur during ORR process [65]. Firstly, the $4e^-$ ORR is a competitive reaction with more positive standard electrode potential than of $2e^-$ ORR process, indicating its thermodynamic favorability. Secondly, the further reduction of H_2O_2 to H_2O may take place at the cathode-solution interface (Eq. 23), or O_2 and H_2O can be produced by disproportionation reaction (Eq. 24), or be oxidized at the anode in the cell, or through the generation of the $HO_2^{\bullet}$ intermediate (Eq. 25) [57,66]. It is generally accepted that the highest yield of H_2O_2 is achieved at pH values

between 2 and 3, with more acidic conditions favoring the reduction of H^+, while the lack of protons with increasing pH reduces the rate of the reaction [67,68].

$$H_2O_2 + 2H^+ + 2e^- \rightarrow 2H_2O \quad (23)$$

$$H_2O_2 \rightarrow O_2 + H_2O \quad (24)$$

$$H_2O_2 \rightarrow HO_2^{\bullet} + H^+ + e^- \rightarrow O_2 + 2H^+ + 2e^- \quad (25)$$

In conclusion, both the selectivity and activity of ORR depend on the adsorption mode and binding energy of O_2 molecules on the electrode surface. Moderate binding energy and Pauling adsorption are beneficial to the production of H_2O_2 *via* $2e^-$ ORR pathway. Therefore, we can modify the structure and composition of electrodes, adjust the adsorption mode and binding energy of O_2 molecules, to achieve an efficient $2e^-$ ORR pathway. Besides, it is necessary to design electrodes and devices to make the generated H_2O_2 diffuse rapidly to avoid further oxidation or reduction.

4. Cathodes in heterogeneous electro-Fenton process for H_2O_2 generation

Generally, in order to increase the production of H_2O_2 in heterogeneous EF process, it is critical to developing suitable cathode materials with excellent $2e^-$ ORR catalytic performance. The cathode materials should have high catalytic activity, good stability, high conductivity, high specific surface area and so on [69,70]. In addition, the performance of electrocatalyst is the key factor, has a great influence on the production yield of H_2O_2 from $2e^-$ ORR process. In recent years, many researchers have devoted to the development of electrocatalysts with high activity and selectivity of $2e^-$ ORR *via* introducing heteroatoms (N, B, S, O, F) and transition metals [71–74].

4.1. Carbon-based electrodes

Carbon-based materials are most widely used in EF system, including carbon felt (CF), activated carbon fiber (ACF), carbon nanotube (CNT) and ordered mesoporous carbon (MOC) [2,9,12,75]. Carbon materials generally have a large specific surface area, high stability, strong electrical conductivity and high hydrogen evolution reaction overpotential, which can provide more active sites for ORR. CF is one of the best candidate materials for the removal of persistent organic pollutants due to its low cost and stable physical and chemical properties [76]. ACF is considered to be one of the most important nano porous carbon materials, which possess *quasi* three-dimensional structure and high specific surface area [77]. Recently, CNTs have become a research hotspot in the field of $2e^-$ ORR due to their unique properties, such as high surface area, mechanical strength, chemical stability and excellent conductivity [78,79].

Due to the limited catalytic activity of carbon-based cathode, a high potential is required during ORR to produce H_2O_2, leading to low H_2O_2 generation efficiency [80]. Generally, the electrocatalytic activity of carbon materials derived from the electronic modulation of the prevalent conjugated sp^2-sp^2 linkages or the delocalization of π-orbital electrons in their graphitic. The incorporation of heteroatoms can change the localized electronic structure of carbon lattice and produce some positively and negatively charged groups, can refine the spin and charge distribution, greatly improving the hydrophobicity/hydrophilicity and turn the absorbability of key ORR intermediates, leading to an enhanced H_2O_2 production performance.

The heteroatom doping on the cathode surface mainly includes O, N, S, P and F. It has been reported that oxygen-containing functional groups such as quinonyl are the active sites of $2e^-$ ORR. Zhou's research group [81] used the electrochemical oxidation method (cyclic voltammetry, CV) to modify the graphite felt cathode with oxygen-containing functional groups in the voltage range of 0–2 V. The research found that the oxygen-containing functional groups C=O and COOH on the graphite felt were increased by 0.84% and 33.57%, respectively. The amount of accumulated H_2O_2 on the modified electrode is about 2.7 times that of the original electrode. In addition, the oxygen-containing functional groups can facilitate the mass transfer of dissolved dioxygen to the active sites of the electrode and its further absorption to form of O_{2abs}, which can improve the $2e^-$ reduction pathway of ORR [82]. The electron delocalization of N-modified carbon material will change the adsorption status of oxygen on the electrode and thus change its ORR selectivity. Compared with C atom, N atom with higher electronegativity can activate π electrons and cause charge redistribution, which further regulates the electronic properties as well as adsorption capacity for O_2 and its intermediates [83]. Peng *et al.* [84] found that the selectivity of H_2O_2 was volcano trend with N content. Both high and low N contents were not beneficial to the selectivity of H_2O_2. High content of N-functional groups may result in decreased isolated active sites for breakage of O–O bond and then lead to the four electron ORR pathway. Low content of N-functionals leads to the decrease of active sites that beneficial for catalytic activity. Furthermore, the types of the N-functionals including quaternary-N, graphitic-N, pyrrolic-N, pyridinic-N and N-oxide are the critical parameters for the H_2O_2 selectivity *via* $2e^-$ ORR process [53]. Many previous studies have suggested that pyrrolic N species favored the two-electron pathway. In addition, under alkaline conditions, the pyridine-N sites were considered to have a four-electron ORR process due to pyridine-N has delocalized lone pair electrons that can be transferred to anti-bonding orbitals in O_2 and weaken O–O bonds. Under acidic conditions, pyridine-N could be protonated through the formation of N–H bonds, which makes the lone pair electrons occupied, thus hinder the weakening of O–O bonds and turn to the two-electron pathway to generate H_2O_2 [63,85]. Zhang *et al.* [86] investigated the use of N-doped carbon derived from covalent organic frameworks with tunable N species and well-defined porous structure for electrocatalytic H_2O_2 production. Based on the control experiments and XPS findings, the graphitic N in N-doped carbons was proved as the active sites for synthesis of H_2O_2 *via* $2e^-$ ORR process. Generally, it is mostly that both specific N and carbon defects are responsible for promoting the $2e^-$ pathway. The doping of B, P, S, F can also regulate the electronegativity of C atoms to favor the generation of active sites for the $2e^-$ ORR. In addition, the heteroatoms doping can change the Fermi level and induce charge polarization, which can regulate the electron transfer characteristics and improve the catalytic activity [68,87].

4.2. The transition metal modified carbon-based electrodes

Transition metal-based materials mainly include metal oxides, metal sulfide, and single metal atom catalyst [88–90]. Compared with noble metals, transition metal-based materials not only have the advantages of high abundance, low cost, environmentally friendly. Besides, the presence of transition metals can facilitate the optimization of absorbate binding, and may enhance the activity and selectivity to generate H_2O_2 [53,87].

Barros *et al.* [88] prepared Fe_3O_4/graphene and Fe_3O_4/Printex carbon electrocatalysts, in which Fe_3O_4 nanoparticles with square shape and average size of 20–30 nm. The number of exchanged electrons was close to 2.7 for the obtained catalysts within the potential range of -0.2 V to -0.7 V *vs.* SCE. Sheng *et al.* [89] used

Table 1
Overview of the studies reported in heterogeneous EF.

Catalysts	Pollutant/concentration	Anode/Cathode	Operational condition	Maximum degradation	Ref.
OCNTs/PBA	Sulfamethazine (50 mg/L)	OCNTs-PBA/Pt	0.05 mol/L Na_2SO_4, pH 6.5, potential -0.5 V (*vs.* SCE)	100% within 30 min	[73]
FeS_2/C	Fluoxetine (10 mg/L)	Carbon cloth/ IrO_2-based plate	neutral pH at 50 mA	91% within 1 h	[95]
Modified iron-carbon	2,4-Dichlorophenol (120 mg/L)	Air diffusion electrode / Ti-IrO_2-RuO_2	0.05 mol/L Na_2SO_4, current intensity 100 mA, pH 6.7	95% within 120 min	[96]
Cu-doped Fe@Fe_2O_3	Tetracycline (20 mg/L)	Cu-doped Fe@Fe_2O_3-CNT-NF/Ti-IrO_2-RuO_2	7.1 g/L Na_2SO_4, 40 mA/cm^2, pH 3	98.1% within 2 h	[97]
AD-Fe/3DPC	Sulfamethoxazole (30 mg/L)	AD-Fe-3DPC/-	0.05 moL/L Na_2SO_4, pH 6, working potential 0.15 V *vs.* RHE	98% within 40 min	[98]
Fe_3C@N-GE-Fe_3O_4	*p*-Ditrosodim -ethylaniline (10 mg/L)	Stainless steel/ Nb-BDD	400 mA, pH 3	91% within 360 min	[99]
CFP@MnO_2-Fe_3O_4/C	Tetracycline (50 mg/L)	CFP@MnO_2-Fe_3O_4-C/BDD	0.1 moL/L Na_2SO_4, 5 mA/cm^2, pH 3	100% at 120 min	[100]
N-doped nano-ZVI@C	Gemfibrozil (10 mg/L)	Carbon-Teflon air-diffusion electrode/Ti-IrO_2	0.05 moL/L Na_2SO_4, 300 mA	95% at 60 min	[105]
FeOx/NHPC	2,4-Dichlorophenol	Carbon paper/platinum sheet	0.05 mol/L Na_2SO_4, pH 6, potential -0.6 V	100% within 120 min	[107]
Fe_2O_3 in CNT	Tetracycline (0.04 mM)	Fe_2O_3-in-CNT/Ti sheet	pH 6.8, flow rate = 1.5 mL/min, 10 mmol/L Na_2SiO_3	97.5% ± 3% within 3 h	[112]
Fe/N-DG	Chloramphenicol (25 mg/L)	Fe-N-DG/Pt	0.05 moL/L Na_2SO_4, pH 13	100% at 210 min	[113]
3DG/Cu@C	Rhodamine B (40 mg/L)	Graphite felt/boron-doped diamond	0.05 mol/L Na_2SO_4, current intensity 30 mA, pH 3	100% within 60 min	[114]
Fe_3O_4/CNT	Carbamazepine (4.7 mg /L)	CMT/Pt- Ti	0.05 moL/L Na_2SO_4, pH 7, 0.9 mA/cm^2	94% ± 3% within 1 h	[116]
Fe_3O_4/N-rGO	Bisphenol A (20 mg/L)	Fe_3O_4-N-rGO/Ti-IrO_2-RuO_2	0.05 moL/L Na_2SO_4, pH 3, 6 mA/cm^2	95% at 90 min	[117]

earth-abundant CoS_2 for the electrocatalytic production of H_2O_2 with the H_2O_2 selectivity of ~70% in ORR process. Density functional theory (DFT) results show that modest bonding of HOO* adsorbate and the kinetically disfavored O-O bond scission leads the high activity and selectivity [91,92]. Single atom catalyst (SAC) is a new research field in the catalysis community, in which the catalytically active metal is exclusively atomically dispersed as a single atom [93]. Sun *et al.* [94] revealed the trend of electrochemical production of H_2O_2 by a series of M-N-C materials (M = Mn, Fe, Co, Ni and Cu). The observation shows that Co-N-C catalyst with outstanding H_2O_2 productivity. The predicted binding energy of HO* intermediate on Co-N-C catalyst is located near the top of a volcano, which is a favorable two-electron ORR.

5. Solid Fenton catalysts in heterogeneous electron-Fenton process for decomposing H_2O_2

Heterogeneous EF process can efficiently expand the pH range of Fenton reaction, overcoming the main drawback of homogeneous Fenton process. Hence, a large variety of heterogeneous Fenton catalyst has been investigated, such as zero valent iron (ZVI), iron oxide, iron sulfide, and loaded iron-based materials [12,46,95–100]. It was found that the reactivity of heterogeneous Fenton reaction depends on the specific surface area, surface charge distribution, and surface functional groups in catalysts [29,46,101,102]. In this part, several common heterogeneous Fenton catalysts are reviewed and their catalytic performance for the degradation of pollutants was discussed and summarized in Table 1.

5.1. Zero valent iron

Zero valent iron (ZVI) received much attention as heterogeneous Fenton catalysts for the degradation of organic compounds [103–105]. In the ZVI Fenton catalytic system, the zero-valent metals are oxidized and then react with H_2O_2 to produce $^{\bullet}OH$. The ZVI surface can be attacked by the following steps: Firstly, O_2 reacts with $\equiv Fe^0$ to form $\equiv Fe^{II}$ in an acidic medium (Eq. 26) or in alkaline conditions (Eqs. 27 and 28). Secondly, the large production of $\equiv Fe^{II}$ potentiates the production of $^{\bullet}OH$ from heterogeneous Fenton's reaction (Eq. 3). Part of Fe^{2+} ion would be generated in acidic medium and then initiated homogeneous Fenton reaction (Eq. 4) [106,107]. The regeneration of $\equiv Fe^{II}$ are achieved through the reducibility of $\equiv Fe^0$ (Eqs. 29 and 30). In addition, it was shown that with the increasing specific surface area more active sites could be *in-situ* generated and consequently both catalytic activity and the reaction rate has been improved in the heterogeneous catalytic process [108,109].

$$\equiv Fe^0 + O_2 + 2H^+ \rightarrow \equiv Fe^{II} + H_2O_2 \quad (26)$$

$$2 \equiv Fe^0 + O_2 + H_2O \rightarrow 2 \equiv Fe^{II} + 4OH^- \quad (27)$$

$$\equiv Fe^0 + 2H_2O \rightarrow \equiv Fe^{II} + 2OH^- + H_2 \quad (28)$$

$$\equiv Fe^0 + 2 \equiv Fe^{III} \rightarrow 3 \equiv Fe^{II} \quad (29)$$

$$\equiv Fe^0 + 2H^+ + H_2O_2 \rightarrow \equiv Fe^{II} + 2H_2O \quad (30)$$

However, ZVI with a large specific surface area would prone to agglomeration during Fenton reaction especially in an aqueous solution. The introduction of support materials such as zeolites, mesoporous silica, carbon nanotubes, and activated carbon is a typical strategy to avoid the ZVI agglomeration [110]. Support materials can effectivity disperse ZVI nanoparticles, increase the specific surface areas, expose more activity sites, and ultimately improve the catalytic activity [110,111]. Zhou's research

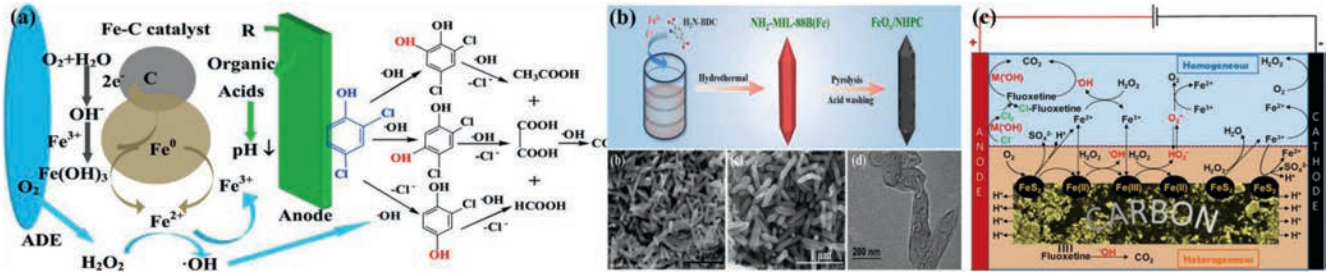

Fig. 3. (a) Degradation pathway and proposed mechanism of 2,4-DCP. Reproduced with permission [95]. Copyright 2015, Elsevier. (b) Scheme of the fabrication process for FeO_x/NHPC, SEM image of NH_2-MIL-88B(Fe), SEM and TEM images of FeO_x/NHPC750. Reproduced with permission [114]. Copyright 2020, Elsevier. (c) Proposed mechanism for FeS_2/C-catalyzed heterogeneous EF treatment at mild pH. Reproduced with permission [96]. Copyright 2020, American Chemical Society.

group [95] used polytetrafluoroethylene modified Fe/C as heterogeneous EF catalyst to degrade 95% of 2,4-dichlorophenol (2,4-DCP) in 120 min under current intensity of 100 mA (Fig. 3a). The connection of carbon particles and iron existed in electrolyte would form a large number of microscopic galvanic cells, in which iron acted as anode and transferred to ferrous ions during Fenton reaction. While support carbon as cathode can accelerate the reduction by transferring electrons and the accepting electrons to the pollutants or oxygen.

5.2. Iron oxide and iron sulfide

In addition to ZVI, iron compounds are attracting much attention as heterogeneous catalysts among the abundantly available materials, such as magnetite (Fe_3O_4), maghemite (γ-Fe_2O_3), feroxyhyte (δ-FeOOH), pyrite (FeS_2) [28–31,112,113]. Niu's team [114] prepared a bifunctional catalyst with embedded FeO_x nanoparticles into nitrogen-doped hierarchically porous carbon (FeO_x/NHPC, Fig. 3b). By adjusting the N-doped configurations and contents, FeO_x/NHPC showed excellent EF properties for degradation and mineralization of 2,4-dichlorophenol, rhodamine B, atrazine, sulfamethoxazole and phenol in a neutral reaction solution. Zhang and Yang [38] found that the degradation of Rhodamine B (RhB) by supported FeOOH nanoparticles as heterogeneous EF catalyst showed a synchronous effect of electrocatalytic oxidation and coupled adsorption, the removal rate of RhB was 100% within 60 min. Özcan *et al.* [115] used Fe_2O_3 modified kaolin (Fe_2O_3-KLN) as catalyst to electrochemically oxidize enrofloxacin (ENXN) by heterogeneous EF process and the degradation rate constant of ENXN was determined as 1.24 ($\pm$0.04) $\times$ 10^9 L mol^{-1} s^{-1}.

Magnetite gave much attention to in heterogeneous EF process. The presence of ferrous ions in magnetite is beneficial to initiate Fenton reaction via Haber-Weiss mechanism [116,117]. In addition, the electron mobility in the spinal structure of magnetite is high enough to enhance the activity of Fenton reaction [35,118]. Liu *et al.* [75] designed a flexible bifunctional nano electrocatalytic textile material (Fe_3O_4-NP@CNF) as heterogeneous EF cathode to degrade carbamazepine. Fe_3O_4 nanoparticles were loaded on the CNT textile which was highly dispersed on the whole fiber matrix. Fe_3O_4-NP@CNF exhibited efficient degradation performance of carbamazepine, which was completely mineralized within 3 h at pH=7.

Pyrite (FeS_2) as one of the most abundant sulfide minerals found in the earth crust has been explored for heterogeneous EF processes [119]. The natural pyrite is both iron reagent and pH regulator. In the presence of O_2, FeS_2 can be oxidized with the accumulation of H^+ in the solution. The corresponding mechanism is shown in the following (Eqs. 31–34) [120]. Ye *et al.* [96] prepared a FeS_2 core-shell nanoparticles as Fenton catalyst to degrade urban wastewater containing fluoxetine, which can be completely removed at near-neutral pH after 60 min (Fig. 3c). Core-shell FeS_2 nanoparticles provided active sites and nanoporous carbon for minimizing the mass transfer limitations and preventing excessive iron leaching. Ammar *et al.* [119] used pyrite power as the source of iron catalyst to degrade tyrosyl (TY), 76% mineralization was obtained after 6 h at 50 mA, and the high performance was due to self-regulation of soluble Fe^{2+} and adjustable pH by pyrite.

$$2FeS_2 + 7O_2 + H_2O \rightarrow 2Fe^{2+} + 4SO_4^{2-} + 4H^+ \quad (31)$$

$$2FeS_2 + 14H_2O_2 \rightarrow 2Fe^{2+} + 4SO_4^{2-} + 14H_2O + 2H^+ \quad (32)$$

$$FeS_2 + 14Fe^{3+} + 8H_2O \rightarrow 15Fe^{2+} + 2SO_4^{2-} + 16H^+ \quad (33)$$

$$CuFeS_2 + 16Fe^{3+} + 8H_2O \rightarrow Cu^{2+} + 17Fe^{2+} + 2SO_4^{2-} + 16H^+ \quad (34)$$

5.3. Iron-free Fenton catalysts

Recently, Fenton-like catalysts have been widely developed, such as Al, Mn, Co, Cu, Ru and Ag existing at least two oxidation states, to attain the efficient degradation of organic wastewater [121]. Cu-based catalysts are widely studied due to the Cu^{2+} reduction by H_2O_2 (4.6 $\times$ 102 L mol^{-1} s^{-1}) is much easier than that in Fe-based redox system, and the reaction rate of Cu^+ with H_2O_2 (1 $\times$ 104 L mol^{-1} s^{-1}) is higher than Fe^{2+} with H_2O_2 (76 L mol^{-1} s^{-1}), which favors the production of $^{\bullet}OH$ [122,123]. Yang *et al.* [123] synthesized a 3DG/Cu@C catalyst to effectively remove a variety of persistent organic pollutants in a wide pH range, the mineralization rate of RhB can reach 81.5%. In addition, the electro-generated H_2O_2 was decomposed by surface $\equiv Cu^{I}$ to generate $^{\bullet}OH$ (Eq. 35), and generated $\equiv Cu^{II}$ existed on the surface of catalysts can be reduced and regenerates $\equiv Cu^{I}$ (Eq. 36). Based on the identification of $O_2^{\bullet-}$ and $^{\bullet}OH$ radicals, an oxidation pathway coupling anodic oxidation with heterogeneous EF was proposed (Fig. 4).

$$\equiv Cu^{I} + H_2O_2 \rightarrow \equiv Cu^{II} + {}^{\bullet}OH + OH^- \quad (35)$$

$$\equiv Cu^{II} + H_2O_2 \rightarrow \equiv Cu^{I} + HO_2^{\bullet} + H^+ \quad (36)$$

Comparing with the copper-based Fenton-like catalysts, manganese is more abundant in valence (0 ~ +7), the oxidation states of +2 to +4 have catalytic properties and environmental applications [121]. Both Mn^{2+} and Mn^{4+} can initiate the decomposition of H_2O_2 by interconversion of intermediate Mn^{3+} substance (Eqs. 37–40) [124,125]. The reaction between H_2O_2 and heterogeneous manganese oxides (MnO, Mn_3O_4, MnOOH and MnO_2) has been intensely investigated for AOP applications.

Depending on the chemical composition (mixed phase or pure phase), physical form (supported or unsupported), the decomposition of H_2O_2 generates different types of ROS including $^{\bullet}OH$

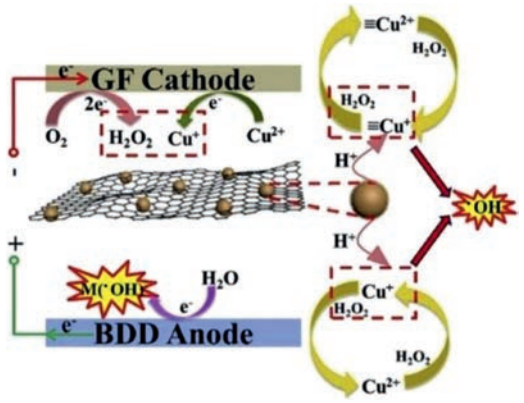

Fig. 4. Proposed mechanism of RhB degradation using 3DG/Cu@C as catalyst in heterogeneous EF process. Reproduced with permission [123]. Copyright 2020, Elsevier.

and superoxide ($O_2^{\bullet-}$) [45,126]. Mi *et al.* [127] have been successfully synthesized a mesoporous $MnCo_2O_4$-CF cathode to degrade ciprofloxacin, the removal of CIP achieved to 100% within 5 h. Compared with MnO_2 andCo_3O_4, $MnCo_2O_4$-CF cathode exhibited higher degradation efficiency of CIP due to the synergistic effect of Mn and Co, enhanced redox couple and accelerated electron transfer.

$$\equiv Mn^{II} + H_2O_2 \rightarrow \equiv Mn^{III} + {}^{\bullet}OH + OH^- \quad (37)$$

$$\equiv Mn^{III} + {}^{\bullet}OH \rightarrow \equiv Mn^{IV} + OH^- \quad (38)$$

$$\equiv Mn^{III} + H_2O_2 \rightarrow \equiv Mn^{II} + HO_2^{\bullet} + H^+ \quad (39)$$

$$\equiv Mn^{IV} + H_2O_2 \rightarrow \equiv Mn^{III} + HO_2^{\bullet} + H^+ \quad (40)$$

6. Integral composite cathodes in heterogeneous electro-Fenton process for direct ·OH generation

Various functionalized materials are reported as EF cathodes for efficiently removing pollutants in aquatic environment such as Fe@Fe_2O_3/ACF [128], FeOOH/GF [129], CoFe-LDH/CF [130]. However, these functionalized EF cathodes were mainly fabricated on the conductive materials or immobilized iron source via multi-fabrication steps. The dissolution, agglomeration and fall off of supported catalysts would result in the decrease of degradation efficiency during EF reaction [36,131]. To overcome these drawbacks, the integrated cathode based on carbon materials has been developed, in which the electrogeneration of H_2O_2 *via* two-electron pathway of oxygen reduction and the onsite decomposition H_2O_2 into ·OH radicals would be simultaneously occurred at the same interface of the intergraded cathode [24,132–134]. Thus, how to achieve the high catalytic performance of $2e^-$ ORR for H_2O_2 generation and $1e^-$ H_2O_2 reduction would be the key parameters for ·OH formation with integrated cathodes in EF process.

Xiao *et al.* [135] reported the selective electrochemical reduction of O_2 to ·OH through $3e^-$ pathway with carbon aerogel encapsulated FeCo alloy (Fig. 5a). The surface –COOH groups on graphite shell serves as the important role to induce the formation of H_2O_2 *via* the two-electron ORR. Simultaneously, H_2O_2 intermediate would be electrocatalytic reduced to ·OH by one-electron on the graphite shell enriched with electrons coming from inner FeCo alloy. The new strategy of electrocatalytic reduction of O_2 to generate ·OH overcomes the rate-limiting step of electron transfer initiated by reduction/oxidation-state cycle in Fenton process. Shen *et al.* [132] proposed a novel electrocatalytic model for the generation of ·OH *via* (2 + 1) e^- oxygen reduction process (Fig. 5b). The

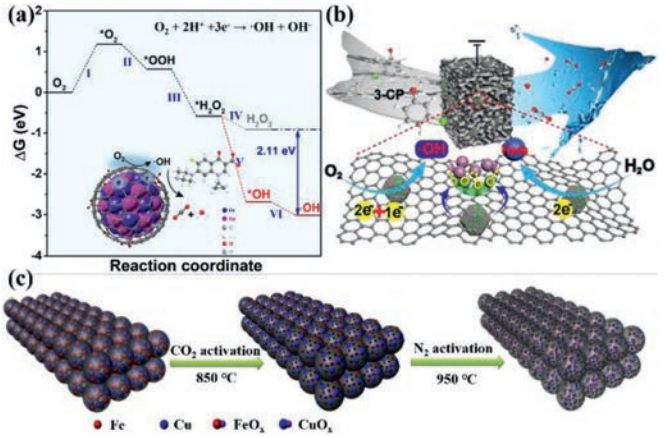

Fig. 5. (a) The thermodynamic activity of O_2 reduction over FeCoC with –COOH and electron transfer mechanism. Reproduced with permission [135]. Copyright 2021, Wiley. (b) Proposed electron transfer mechanism of PdFe alloy/CA as catalyst in heterogeneous EF process. Reproduced with permission [132]. Copyright 2020, American Chemical Society. (c) Schematic illustration of the sequential activation of FeCuC aerogel by CO_2 and N_2. Reproduced with permission [131]. Copyright 2016, American Chemical Society.

PdFe alloy is dispersed in the carbon aerogel matrix, favoring the formation of carbon defects. Different from the $3e^-$ oxygen reduction pathway, the electrogenerated intermediate H_2O_2 was decomposed by PdFe alloy. Specifically, PdFe nanoalloys promote the generation of $[H]_{ads}$ as reduction sites for removing haloacetamides in drinking water.

The regeneration of Fe^{II} would be the rate-determing step in $1e^-$ H_2O_2 reduction reaction that initiated by reduction/oxidation-state cycle during EF process. Tian *et al.* [134] designed a novel Fe-sulfur doped carbon aerogel (FeSCA) cathode. The unsaturated surface sulfur accelerates the transformation of Fe^{III}/Fe^{II}. In addition, the evenly distributed sulfur favors the formation of –COOH groups to improve the selectivity of $2e^-$ oxygen reduction. Liu *et al.* [24] found that by boosting internal electron transfer to a nitrogen-conjugated Fe^{III} complex can accelerate the Fe^{II} regeneration in the EF process.

The catalytic activity of Fenton active sites in integrated cathode would be improved by the environmentally friendly activation way with CO_2 and N_2. Zhao *et al.* [131] prepared an iron-copper integrated carbon aerogel (FeCuC) cathode, in which ultradispersed Fe^0 and Cu^0 nanoparticles were embedded in 3D carbon matrix (Fig. 5c). The CO_2 activation enhanced the accessibility of the aerogel's pores, and the secondary activation of N_2 increased the porosity of aerogels and reductive carbon to regenerate ultradispersed Fe^0. The activated FeCuC integrated cathode exhibited high Fenton catalytic activity and excellent stability in a wide pH range (3–9), the removal efficiency for methylene blue reached 98% within 30min.

7. The applications of heterogeneous electro-Fenton process for degradation contaminants of emerging concerns

7.1. Degradation of pesticide

There are about 600 kinds of synthetic chemical pesticides, such as organochlorine, chlorophenoxy compounds, aniline derivatives [136]. Many pesticides are responsible for hypertension, cardiovascular disorders and other health-related problems in humans. The existence of pesticides in aquatic system and drinking water is a common occurrence, which is due to the leaching of pesticides from agricultural runoffs and industrial discharge into groundwater. Recently, heterogeneous EF technology serves as an

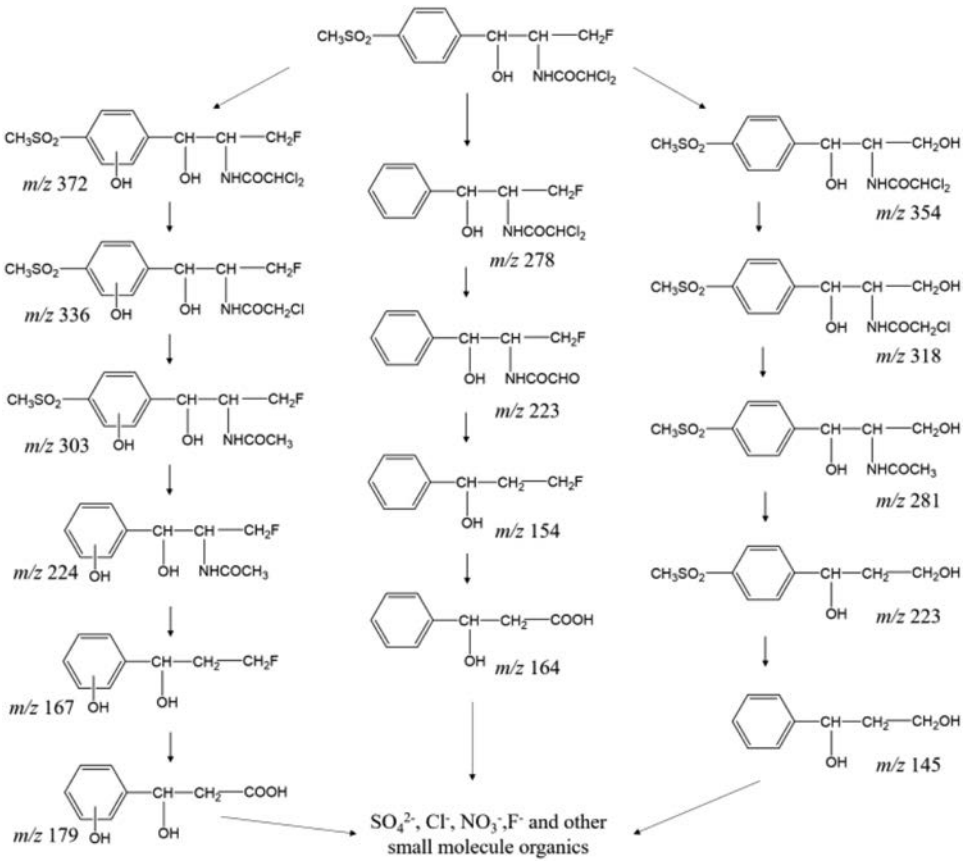

Fig. 6. Possible degradation pathways of florfenicol in heterogeneous EF process with EFCM. Reproduced with permission [140]. Copyright 2018, American Chemical Society.

attractive alternative way to deeply remove pesticides in municipal wastewater, Wang *et al.* [137] used electro-Fenton system with Fe-based magnetic activated carbon to degrade herbicide diuron. For 10 mg/L diuron solution, it can be completely degraded in 120 min at pH 6.7. Zhao *et al.* [131] applied EF process with FeCuC integrated as cathode and boron-doped diamond as anode to degrade the imidacloprid. 88% total organic carbon (TOC) removal was reached in 4h at a wide pH range.

7.2. Degradation of antibiotics

Antibiotics are a class of pharmaceuticals used to treat bacterial and fungal infections both for human and animal [138]. Due to the inefficient removal of antibiotics in traditional sewage treatment plants, their long-term existence and migration in the environment pose a potential threat to aquatic organisms and human life [7,139]. During the natural degradation process, such as hydrolysis, biodegradation and photo-degradation, antibiotics will react with other organic substances and convert to more complex by-products. Therefore, it is necessary to treat antibiotics to avoid surface water pollution and production of toxic by-products before they are released to natural water [140]. EF technology is new advanced oxidation technology that has been developed in recent decades, showing high efficiency of antibiotics oxidation [141,142].

Jiang *et al.* [140] prepared an electro-Fenton catalytic membrane (EMFC) modified by graphene and iron oxide particles on a polytetrafluoroethylene substrate for *in-situ* degradation of antibiotic florfenicol with 10.2 ± 0.1 mg m^{-2} h^{-1} removal rate (Fig. 6). The degradation mechanisms of florfenicol were *via* the formation of several intermediates, undergo desulfuration, defluorination, and dehalogenation oxidation reactions which were later mineralized to CO_2 and other different inorganic ions. Plakas *et al.* [139] reported the 85% diclofenac removal and corresponding 36% TOC removal in EF process with modified carbon felt with iron oxide at the applied potential of 2 V. This performance is considered satisfactory because the EF process occurs under unfavorable conditions of presence of natural organic matter and low electrical conductivity in real waste water.

7.3. Degradation of endocrine disrupting chemicals

Endocrine disrupting chemicals (EDCs) have been received significant attention due to their widely presence in environment, such as bisphenol A, phenols, phthalates. EDCs pollution can cause health issues by imitating or inhibiting the biology metabolic activities of the endocrine system [3,4]. The removal of EDCs including activating carbon adsorption, membrane filtration, biological approach, photocatalytic oxidation were widely reported in the previous literatures. The heterogeneous EF is one of the promising ways due to its high pollutant's degradation and mineralization efficiency [143–146].

Liu *et al.* [75] used the composite binder-free Fe_3O_4-NP@CNF textile to generate H_2O_2 through O_2 reduction. The TOC removal efficiency reached about 95% after 150 min, under the condition of pH 7. The results show that this process can remove carbamazepine with minimal energy consumption (0.239 kWh/g) and high *pseudo*-first-order rate constants (6.85 h^{-1}). Zhang *et al.* [117] prepared a novel three-dimensional (3D) heterogeneous EF system with magnetic nitrogen doped/reduced graphene oxide as catalytic particle electrodes and improved gas diffusion electrode as cathode for Bisphenol A (BPA) removal. The removal rate of BPA and TOC was respectively 93% and 60.5% within 90 min, and low catalyst loss after 5 cycles (less than 9.5%), indicating its excellent reusability and stability.

8. Conclusion and prospect

Heterogeneous EF is an efficient and environmentally friendly technology for wastewater treatment owing to its high applicability over a wide pH range, in which the H_2O_2 is *in-situ* formed by two-electron oxygen reduction reaction. The desirable features for potential cathodes and catalysts in EF process include high catalytic activity of cathodes for generation and activation of electrogenerated H_2O_2, as well as the easy separation and reusability of Fenton catalysts. In this review, the surface catalytic mechanism of heterogeneous EF reaction, electrocatalytic formation of H_2O_2 *via* $2e^-$ ORR, the generation of $^{\bullet}OH$ with solid catalysts and integrated cathodes, as well as the application of EF in the treatment of various pollutants sewage were summarized in detail. Heterogeneous EF reaction consists of the Haber-Weiss circle mechanism depending on the different working pH may accompany the dissolved M^n/M^{n+1} released from the solid catalyst. The selectivity and activity of $2e^-$ ORR depend on the adsorption mode and binding energy of O_2 molecules on the electrode surface. Moderate binding energy and Pauling adsorption are beneficial to the production of H_2O_2. The activity of heterogeneous iron-based Fenton catalyst can be effectivity enhanced by increasing specific surface area and dispensability, and exposing more active sites. The regeneration of Fe^{II} can be accelerated through interface electronic transfer and circulation by introducing bimetallic catalyst, inorganic ligands and electrochemical reduction. Inorganic metal compounds have been used to introduce a thermodynamically spontaneous Fe^{II} regeneration *via* the synergistic effect of Fe and other metals with different redox potentials. The applications of heterogeneous EF process are widely reported for the complete degradation and mineralization of wastewater contaminated with different classes of organic pollutants. In order to meet highly competitive requirement of actual wastewater treatment in the future, the spotlight of heterogeneous EF technology should be put in following aspects.

(i) The main challenges encountered in heterogeneous EF reaction are the limited Fenton activity. Due to the unique electronic properties of single metal active site, the atomically distributed active metal center has become a new research frontier to obtain the maximum atom efficiency in recent years. However, there are few studies on single atom catalysts as heterogeneous Fenton catalysts and it worth to be investigated in heterogeneous EF process for improving the catalytic activity of Fenton reaction during the degradation of organic pollutants.

(ii) The efficiency of EF process is highly dependent on the synthesis of H_2O_2. However, development of electrochemical production of H_2O_2 is still challenging because of the low H_2O_2 yield and unsatisfactory Faradaic efficiency mainly deriving from the catalytic activity and selectivity of catalysts. And only a few implementations of practical devices for H_2O_2 production and water treatment exist, all of which involve low efficiencies and complex designs. Thus, improvements to catalyst and reactor designs are necessary for commercialization.

(iii) The scavenging effect of $^{\bullet}OH$ by natural organic matters and inorganic ions in real wastewater leads a large amount of energy to be consumed and unsatisfactory reduction of targeting pollutants. Besides, $^{\bullet}OH$-mediated heterogeneous EF process can nonselectively eliminate the recalcitrant organic pollutants. Specially, the selective removal of targeting pollutants with low concentration and high toxicity during the treatment of actual wastewater is challenging, which will undoubtedly broaden the application prospect of heterogeneous EF process.

Declaration of competing interest

The authors declare that they have no known competing financial interests or personal relationships that could have appeared to influence the work reported in this paper.

Acknowledgments

The authors acknowledge funding from the National Natural Science Foundation of China (Nos. 22076142, 21677106, 22076140), National Key Basic Research Program of China (No. 2017YFA0403402), National Natural Science Foundation of China (No. U1932119), the Science & Technology Commission of Shanghai Municipality (No. 14DZ2261100), the Fundamental Research Funds for the Central Universities.

References

[1] G. Chen, Y. Gao, G. Zhu, et al., Chin. Chem. Lett. 31 (2020) 2730–2736.
[2] J. Yang, D. Zeng, Q. Zhang, et al., Appl. Catal. B 279 (2020) 119363.
[3] J. He, X. Yang, B. Men, L. Yu, D. Wang, J. Mol. Catal. A: Chem. 408 (2015) 179–188.
[4] X. Hu, B. Liu, Y. Deng, et al., Appl. Catal. B 107 (2011) 274–283.
[5] X. Hu, Y. Deng, J. Zhou, et al., Sep. Purif. Technol. 251 (2020) 117376.
[6] Y. Zhang, A. Wang, S. Ren, et al., Chemosphere 221 (2019) 423–432.
[7] X. Liu, Y. Zhou, J. Zhang, et al., Chem. Eng. J. 347 (2018) 379–397.
[8] J. Du, B. Zhang, J. Li, B. Lai, Chin. Chem. Lett. 31 (2020) 2575–2582.
[9] S.O. Ganiyu, M. Zhou, C.A. Martínez-Huitle, Appl. Catal. B 235 (2018) 103–129.
[10] L. Pi, J. Cai, L. Xiong, et al., Chem. Eng. J. 389 (2020) 123420.
[11] W. Xiang, M. Huang, Y. Wang, X., et al., Chin. Chem. Lett. 31 (2020) 2831–2834.
[12] S. Liu, L. Mei, X. Liang, et al., ACS Appl. Mater. Inter. 10 (2018) 29467–29475.
[13] G. Wang, D. Zhao, F. Kou, et al., Chem. Eng. J. 351 (2018) 747–755.
[14] A. Kumar, A. Rana, G. Sharma, et al., J. Mol. Liq. 290 (2019) 111177.
[15] Z.H. Liu, Z. Dang, Y. Liu, Environ. Sci. Pollut. Res. Int. 28 (2021) 19505–19510.
[16] J. Scaria, A. Gopinath, P.V. Nidheesh, J. Clean. Prod. 278 (2021) 124014.
[17] A. Afzal, P. Drzewicz, L.A. Perez-Estrada, et al., Environ. Sci. Technol. 46 (2012) 10727–10734.
[18] M.M.E. Popov, D. Santoro, L. Liberti, J. Eloranta, Environ. Sci. Technol. 44 (2010) 7827–7832.
[19] G.R. Pophali, S. Hedau, N. Gedam, N.N. Rao, T. Nandy, J. Hazard. Mater. 189 (2011) 273–277.
[20] K.E. O'Shea, D.D. Dionysiou, J. Phys. Chem. Lett. 3 (2012) 2112–2113.
[21] J. Li, Y. Li, Z. Xiong, G. Yao, B. Lai, Chin. Chem. Lett. 30 (2019) 2139–2146.
[22] C. Wang, Y. Liu, T. Zhou, et al., Chin. Chem. Lett. 30 (2019) 2231–2235.
[23] E. Brillas, C.A. Martínez-Huitle, Appl. Catal. B 166 (2015) 603–643.
[24] M. Liu, Z. Feng, X. Luan, et al., Environ. Sci. Technol. 55 (2021) 6042–6051.
[25] L. Guo, F. Chen, X. Fan, W. Cai, J. Zhang, Appl. Catal. B 96 (2010) 162–168.
[26] P.V. Nidheesh, R. Gandhimathi, Desalination 299 (2012) 1–15.
[27] S. Lu, L. Liu, H. Demissie, G. An, D. Wang, Environ. Int. 146 (2021) 106273.
[28] S. Song, H. Yang, R. Rao, H. Liu, A. Zhang, Appl. Catal. A: Gen. 375 (2010) 265–271.
[29] M. Hermanek, R. Zboril, Medrik, et al., J. Am. Chem. Soc. (2007) 10929–10935.
[30] J. Zhuang, K. Fan, L. Gao, et al., Mol. Pharm. 9 (2012) 1983–1989.
[31] X. Zuo, C. Peng, Q. Huang, et al., Nano Res. 2 (2009) 617–623.
[32] V. Poza-Nogueiras, E. Rosales, M. Pazos, M.A. Sanroman, Chemosphere 201 (2018) 399–416.
[33] J. Meijide, P.S.M. Dunlop, M. Pazos, M.A. Sanromán, Catalysts 11 (2021) 85.
[34] I.S.E. Brillas, M.A. Oturan, Chem. Rev. 12 (2009) 6570.
[35] M. Munoz, Z.M. Pedro, J.A. Casas, J.J. Rodriguez, Appl. Catal. B 176 (2015) 249–265.
[36] Y. Wang, G. Zhao, S. Chai, H. Zhao, Y. Wang, ACS Appl. Mater. Interfaces 5 (2013) 842–852.
[37] Z. Wan, J. Wang, J. Hazard. Mater. 324 (2017) 653–664.
[38] G. Zhang, F. Yang, J. Electrochem. Soc. 6 (2015) H357–H365.
[39] A.L. Pham, F.M. Doyle, D.L. Sedlak, Environ. Sci. Technol. 46 (2012) 1055–1062.
[40] H. Zhao, Y. Wang, Y. Wang, T. Cao, G. Zhao, Appl. Catal. B 125 (2012) 120–127.
[41] W.Ma J.Ma, W. Song, Environ. Sci. Technol. 40 (2006) 618–624.
[42] W.P. Kwan, B.M. Voelker, Environ. Sci. Technol. 37 (2003) 1150.
[43] Y. Qin, F. Song, Z. Ai, P. Zhang, L. Zhang, Environ. Sci. Technol. 49 (2015) 7948–7956.
[44] S. Mansoori, R. Davarnejad, E.J. Ozumchelouei, A.F. Ismail, J. Water Process Eng. 39 (2021) 101888.
[45] Q. Wang, M. Liu, H. Zhao, et al., Chem. Eng. J. 378 (2019) 122071.
[46] R.C.C. Costa, F.C.C. Moura, J.D. Ardisson, J.D. Fabris, R.M. Lago, Appl. Catal. B 83 (2008) 131–139.

[47] F. Moura, G. Oliveira, M. Araujo, et al., Appl. Catal. A: Gen. 307 (2006) 195–204.
[48] R. Yang, Y. Zhou, Y. Xing, et al., Appl. Catal. B 253 (2019) 131–139.
[49] G. Divyapriya, I.M. Nambi, J. Senthilnathan, Chem. Eng. J. 316 (2017) 964–977.
[50] B.Q. Li, C.X. Zhao, J.N. Liu, Q. Zhang, Adv. Mater. 31 (2019) 1808173.
[51] B.Q. Li, C.X. Zhao, S. Chen, et al., Adv. Mater. 31 (2019) 1900592.
[52] Y.J. Sa, D.J. Seo, J. Woo, et al., J. Am. Chem. Soc. 138 (2016) 15046–15056.
[53] Y. Wang, G.I.N. Waterhouse, L. Shang, T. Zhang, Adv. Energy Mater. 11 (2020) 2003323.
[54] A. Verdaguer-Casadevall, D. Deiana, M. Karamad, et al., Nano Lett. 14 (2014) 1603–1608.
[55] J.H. Zagal, M.T. Koper, Angew. Chem. Int. Ed. 55 (2016) 14510–11452.
[56] K. Wang, J. Huang, H. Chen, Y. Wang, S. Song, Chem. Commun. 56 (2020) 12109–12121.
[57] H.W. Kim, V.J. Bukas, H. Park, et al., ACS Catal. 10 (2019) 852–863.
[58] Y. Sun, L. Han, P. Strasser, Chem. Soc. Rev. 49 (2020) 6605.
[59] G.L. Chai, Z. Hou, T. Ikeda, K. Terakura, J. Phys. Chem. C 121 (2017) 14524–14533.
[60] J. Clavilier, D. Armand, S.G.Sun.M. Petit, J. Electroanal. Chem. 205 (1986) 267–277.
[61] J.S. Jirkovsky, I. Panas, E. Ahlberg, et al., J. Am. Chem. Soc. 133 (2011) 19432–19441.
[62] J.K. Edwards, A. Thomas, A.F. Carley, et al., Green Chem. 10 (2008) 388–394.
[63] J. Zhang, H. Zhang, M. Cheng, et al., Small 16 (2020) 1902845.
[64] Y. Zhou, G. Chen, J. Zhang, et al., J. Mater. Chem. A 8 (2020) 20849–20869.
[65] T. Yu, C.B. Breslin, Materials 13 (2020) 2544.
[66] C.M. Sánchez-Sánchez, A.J. Bard, Anal. Chem. 81 (2009) 8094–8100.
[67] Y. Pang, H. Xie, Y. Sun, M.M. Titirici, G. Chai, J. Mater. Chem. A 8 (2020) 24996–25016.
[68] H. Zhao, Z.Y. Yuan, ChemSusChem 14 (2021) 1616–1633.
[69] Y. Jiang, P. Ni, C. Chen, et al., Adv. Energy Mater. 8 (2018) 1801909.
[70] L. Li, C. Tang, Y. Zheng, et al., Adv. Energy Mater. 10 (2020) 2000789.
[71] H. Yin, Y. Dou, S. Chen, et al., Adv. Mater. 32 (2019) 1904870.
[72] C. Tang, Y. Jiao, B. Shi, et al., Angew. Chem. Int. Ed. 59 (2020) 9171–9176.
[73] S. Cheng, C. Shen, H. Zheng, F. Liu, A. Li, Appl. Catal. B 269 (2020) 118785.
[74] M. Xing, W. Xu, C. Dong, et al., Chem 4 (2018) 1359–1372.
[75] K. Liu, J.C. Yu, H. Dong, et al., Environ. Sci. Technol. 52 (2018) 12667–12674.
[76] M. Pimentel, N. Oturan, M. Dezotti, M.A. Oturan, Appl. Catal. B 83 (2008) 140–149.
[77] C. Trellu, N. Oturan, F.K. Keita, et al., Environ. Sci. Technol. 52 (2018) 7450–7457.
[78] H. Yang, M. Zhou, W. Yang, G. Ren, L. Ma, Chemosphere 206 (2018) 439–446.
[79] J. Peng, Y. He, C. Zhou, S. Su, B. Lai, Chin. Chem. Lett. 32 (2021) 1626–1636.
[80] K.M. Nair, V. Kumaravel, S.C. Pillai, Chemosphere 269 (2021) 129325.
[81] L. Zhou, M. Zhou, C. Zhang, et al., Chem. Eng. J. 233 (2013) 185–192.
[82] H. Zhao, X. Shen, Y. Chen, et al., Chem. Commun. 55 (2019) 6173–6176.
[83] P. Kaur, G. Verma, S.S. Sekhon, Prog. Mater. Sci. 102 (2019) 1–71.
[84] Q. Peng, Z. Zhang, Z.a. Huang, W. Ren, J. Sun, RSC Adv. 4 (2014) 60168–60175.
[85] W. Zhou, X. Meng, J. Gao, A.N. Alshawabkeh, Chemosphere 225 (2019) 588–607.
[86] J. Zhang, G. Zhang, S. Jin, et al., Carbon 163 (2020) 154–161.
[87] K. Dong, Y. Lei, H. Zhao, et al., J. Mater. Chem. A 8 (2020) 23123–23141.
[88] W. Barros, Q. Wei, G. Zhang, et al., Electrochim. Acta 162 (2015) 263–270.
[89] H. Sheng, E.D. Hermes, X. Yang, et al., ACS Catal. 9 (2019) 8433–8442.
[90] Y. Ding, W. Zhou, J. Gao, F. Sun, G. Zhao, Adv. Mater. Interfaces 8 (2021) 2002091.
[91] Z. Song, L. Zhang, K. Doyle-Davis, et al., Adv. Energy Mater. 10 (2020) 2001561.
[92] S. Chen, Z. Chen, S. Siahrostami, et al., ACS Sustain. Chem. Eng. 6 (2017) 311–317.
[93] Y. Chen, S. Ji, C. Chen, et al., Joule 2 (2018) 1242–1264.
[94] Y. Sun, L. Silvioli, N.R. Sahraie, et al., J. Am. Chem. Soc. 141 (2019) 12372–12381.
[95] C. Zhang, M. Zhou, G. Ren, et al., Water Res. 70 (2015) 414–424.
[96] Z. Ye, J.A. Padilla, E. Xuriguera, et al., Environ. Sci. Technol. 54 (2020) 4664–4674.
[97] T. Luo, H. Feng, L. Tang, et al., Chem. Eng. J. 382 (2020) 122970.
[98] P. Cao, X. Quan, K. Zhao, et al., Environ. Sci. Technol. 54 (2020) 12662–12672.
[99] H. Ghanbarlou, B. Nasernejad, M.N. Fini, et al., Chem. Eng. J. 395 (2020) 125025.
[100] P. Dong, X. Chen, M. Guo, et al., J. Hazard. Mater. 412 (2021) 125208.
[101] C. Gregor, M. Hermanek, D. Jancik, et al., Eur. J. Inorg. Chem. 16 (2010) 2343–2351.
[102] P. Robert, H. Martin, Z. Radek, Appl. Catal. A: Gen. 366 (2009) 325–332.
[103] M. Barreto-Rodrigues, F.T. Silva, T.C. Paiva, J. Hazard. Mater. 165 (2009) 1224–1228.
[104] Y.P. Sun, X.Q. Li, J. Cao, W.X. Zhang, H.P. Wang, Adv. Colloid Interface Sci. 120 (2006) 47–56.
[105] Z. Ye, J.A. Padilla, E. Xuriguera, E. Brillas, I. Sirés, Appl. Catal. B 266 (2020) 118604.
[106] J. Bogacki, P. Marcinowski, E. Zapałowska, J. Maksymiec, J. Naumczyk, Environ. Technol. 38 (2016) 2589–2600.
[107] Y. Segura, F. Martínez, J.A. Melero, J.L.G. Fierro, Chem. Eng. J. 269 (2015) 298–305.
[108] A.J. Feitz, S.H. Joo, J. Guan, et al., Colloids Surf. A Physicochem. Eng. Asp. 265 (2005) 88–94.
[109] M. Cao, L. Wang, L. Wang, J. Chen, X. Lu, Chemosphere 90 (2013) 2303–2308.
[110] A. Rodrıguez, G. Ovejero, J.L. Sotelo, M. Mestanza, J. Garcıá, Ind. Eng. Chem. Res. 49 (2010) 498–505.
[111] P. Wang, X. Zhou, Y. Zhang, et al., RSC Adv. 7 (2017) 26983–26991.
[112] D. Guo, Y. Liu, H. Ji, et al., Environ. Sci. Technol. 55 (2021) 4045–4053.
[113] X. Song, H. Zhang, Z. Bian, H. Wang, J. Hazard. Mater. 412 (2021) 125162.
[114] P. Cao, X. Quan, K. Zhao, et al., J. Hazard. Mater. 382 (2020) 121102.
[115] A. Özcan, A.A. Özcan, Y. Demirci, E. Şener, Appl. Catal. B. 200 (2017) 361–371.
[116] M. Mohseni, K. Demeestere, G.D. Laing, et al., Adv. Sustain. Syst. 5 (2021) 2100001.
[117] Y. Zhang, Z. Chen, P. Wu, et al., J. Hazard. Mater. 393 (2020) 120448.
[118] A. Dhakshinamoorthy, S. Navalon, M. Alvaro, H. Garcia, ChemSusChem 5 (2012) 46–64.
[119] S. Ammar, M.A. Oturan, L. Labiadh, et al., Water Res 74 (2015) 77–87.
[120] L. Labiadh, M.A. Oturan, M. Panizza, N.B. Hamadi, S. Ammar, J. Hazard. Mater. 297 (2015) 34–41.
[121] A.D. Bokare, W. Choi, J. Hazard. Mater. 275 (2014) 121–135.
[122] J.F. Perez-Benito, J. Inorg. Biochem. 98 (2004) 430–438.
[123] Y. Yang, Y. Liu, X. Fang, et al., Chemosphere 243 (2020) 125423.
[124] R.J. Watts, J. Sarasa, F.J. Loge, A.L. Teel, J. Environ. Eng. 131 (2005) 158–164.
[125] K.W. Jung, S.Y. Lee, Y.J. Lee, J.W. Choi, Ultrason. Sonochem. 57 (2019) 22–28.
[126] M.Á. Fernández de Dios, E. Rosales, M. Fernández-Fernández, M. Pazos, M.Á. Sanromán, J. Chem. Technol. Biotechnol. 90 (2015) 1439–1447.
[127] X. Mi, Y. Li, X. Ning, et al., Chem. Eng. J. 358 (2019) 299–309.
[128] J. Li, Z. Ai, L. Zhang, J. Hazard. Mater. 164 (2009) 18–25.
[129] M. Sun, X. Ru, L. Zhai, Appl. Catal. B. 165 (2015) 103–110.
[130] S.O. Ganiyu, T.X. Huong Le, M. Bechelany, et al., J. Mater. Chem. A 5 (2017) 3655–3666.
[131] H. Zhao, L. Qian, X. Guan, D. Wu, G. Zhao, Environ. Sci. Technol. 50 (2016) 5225–5233.
[132] X. Shen, F. Xiao, H. Zhao, et al., Environ. Sci. Technol. 54 (2020) 4564–4572.
[133] H. Zhao, Q. Wang, Y. Chen, Q. Tian, G. Zhao, Carbon 124 (2017) 111–122.
[134] Q. Tian, F. Xiao, H. Zhao, et al., Appl. Catal. B 272 (2020) 119039.
[135] F. Xiao, Z. Wang, J. Fan, et al., Angew. Chem. Int. Ed. 60 (2021) 2–11.
[136] J. Senthilnathan, S.A. Younis, E.E. Kwon, et al., J. Hazard. Mater. 400 (2020) 123323.
[137] X. Wang, K. Zhu, X. Ma, Z. Sun, X. Hu, RSC Adv. 8 (2018) 19971–19978.
[138] K. Kummerer, Chemosphere 75 (2009) 417–434.
[139] K.V. Plakas, S.D. Sklari, D.A. Yiankakis, et al., Water Res. 91 (2016) 183–194.
[140] W.L. Jiang, X. Xia, J.L. Han, Environ. Sci. Technol. 52 (2018) 9972–9982.
[141] A.R. Ribeiro, B. Sures, T.C. Schmidt, Environ. Pollut. 241 (2018) 1153–1166.
[142] A.L. Estrada, Y.Y. Li, A. Wang, J. Hazard. Mater. 227-228 (2012) 41–48.
[143] B. Lei, S. Huang, Y. Zhou, D. Wang, Z. Wang, Chemosphere 76 (2009) 36–42.
[144] S.Y. Wee, A.Z. Aris, Environ. Int. 106 (2017) 207–233.
[145] Q. Yang, Z. Feng, M. Liu, et al., Chin. Chem. Lett. (2021), doi:doi.org/10.1016/j.cclet.2021.05.066.
[146] J. Zhao, Z. Zhang, X. Chen, et al., Acta Chim. Sin. 78 (2020) 961–967.